arXiv:0804.0617v1 [cond-mat.str-el] 3 Apr 2008

Excitons in the One-Dimensional Hubbard Model: a Real-Time Study

K. A. Al-Hassanieh,[1] F. A. Reboredo,[2] A. E. Feiguin,[3,4] I. González,[2,5] and E. Dagotto[2,5]

[1]*Theoretical Division T-11, Los Alamos National Laboratory, Los Alamos, NM 87545, USA*
[2]*Materials Science and Technology Division, Oak Ridge National Laboratory, Oak Ridge, TN 37831, USA*
[3]*Condensed Matter Theory Center, Department of Physics, The University of Maryland, College Park, MD 20742, USA*
[4]*Microsoft Project Q, The University of California, Santa Barbara, CA 93106, USA*
[5]*Department of Physics and Astronomy, The University of Tennessee, Knoxville, TN 37996, USA*

We study the real-time dynamics of a pair hole/doubly-occupied-site, namely a holon and a doublon, in a 1D Hubbard insulator with on-site and nearest-neighbor Coulomb repulsion. Our analysis shows that the pair is long-lived and the expected decay mechanism to underlying spin excitations is actually inefficient. For a nonzero inter-site Coulomb repulsion, we observe that part of the wave-function remains in a bound state. Our study also provides insight on the holon-doublon propagation in real space. Due to the one-dimensional nature of the problem, these particles move in opposite directions even in the absence of an applied electric field. The potential relevance of our results to solar cell applications is discussed.

PACS numbers: 71.10.-w, 71.10.Fd, 71.35.-y, 71.35.Cc

Introduction. In most band insulators and semiconductors, a single particle picture is sufficient for a qualitative grasp of transport and optical properties. This simplicity was crucial for an early understanding of their electronic structure and for discoveries, such as the transistor and semiconductor solar cells. An equivalent progress for strongly correlated electronic materials (SCEM), such as Mott-Insulators, has marched at a slower pace since complicated many-body interactions govern their behavior, and the one-electron picture breaks down [1]. Nevertheless, gigantic optical nonlinear properties, potentially useful for applications, have been reported in 1D Mott-Hubbard materials, such as Sr_2CuO_3 [2]. However, the majority of SCEM research has focused on fundamental science issues. While interesting technologies might emerge as a result of the exotic transport properties and complex phase diagrams of SCEM [3], their optical properties have been largely regarded only as a probe of the ground state. Whether SCEM can be of use for applications in solar cells, photo-catalysis or solid-state-lighting devices will depend on our basic understanding of their optical properties and specifically on the dynamics of the optical excitations.

The market of light-to-energy conversion is currently dominated by semiconductor materials, silicon in particular. Composite tandem solar cells have been fabricated to take maximum advantage of the solar spectra [4]. However, semiconductor solar cells are very sensitive to defects in the crystal lattice, which implies that cost remains a major limiting factor [5]. Current efforts to reduce the cost of solar cells include the exploration of other alternatives such as composites of polymers, quantum dots, and their combinations [6]. In these novel devices, excitons dissociate into electrons and holes at the interface of two materials with different band offsets.

It is frequently claimed that to date "all photo voltaic technologies use semiconductor materials" [7]. While ideal solar cell materials have to fulfill a number of properties [8], note that having a gap between 1.1 and 1.7 eV, of *any* origin, is the basic requirement. The fact that photo-catalytic processes are not quenched in composites involving manganites [9] raises hope for many highly correlated oxides to be technologically useful for light-to-energy conversion. To control the values of their potentially useful intrinsic gaps, transition metal oxides can be grown in complex layered super-lattices [10, 11].

However, one can argue against these highly correlated oxides as candidates for solar energy harvesting materials since the optical gap arises only as a result of electronic correlations: they would be metallic otherwise. As a result, the ground state is magnetic with low-energy excitations, which in principle can provide a path for the exciton decay. Excitons in SCEM have received much theoretical attention [12, 13], but most of the efforts have focused on the exciton formation and its properties. They have also been observed experimentally in 1D Mott insulators [14]. A real-time study of the excitation propagation in real-space, accounting for its decay in addition to the bound state formation, has not been presented before to our knowledge.

In this Letter, we study the dynamics of holon-doublon excitations in the 1D extended Hubbard model using the recently developed time-dependent density-matrix renormalization group (TDDMRG). We find that: (i) The mechanism for exciton decay into magnetic excitations is very inefficient and the pair holon/doublon is long-lived. This suggests that 1D SCEM can in principle be used to generate power or promote chemical reactions at the surface, adding to its previously discussed potential role as optical switches [2]; (ii) at least in quasi-1D systems, despite the absence of an electric field, the holon and doublon move in opposite directions even in the presence of a finite attraction; (iii) in agreement with previous calculations, a fraction of the pair forms a bound state.

Model and Technique. We investigate an open Hubbard chain of L sites with on-site and nearest-neighbor (NN) Coulomb repulsion. The number of electrons is set to L, i.e. the system is at half-filling. The Hamiltonian is given by

$$\hat{H} = -t_h \sum_{\sigma,i=1}^{L-1} (c^\dagger_{i\sigma} c_{i+1\sigma} + H.c.) + U \sum_{i=1}^{L} (\hat{n}_{i\uparrow} - \frac{1}{2})(\hat{n}_{i\downarrow} - \frac{1}{2})$$

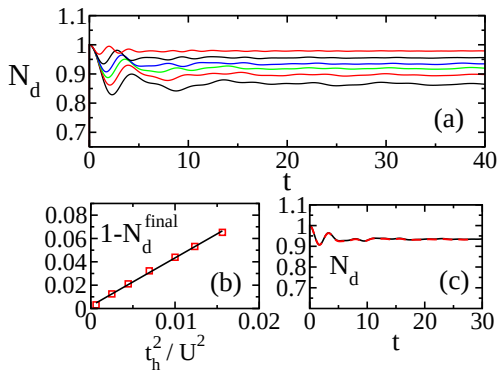

FIG. 1: Decay of the holon-doublon excitation. (a) Time-evolution of the total double occupation N_d for $V = 0$ and $U/t_h = 5, 6, 7, 8, 10$, and 15 (bottom to top). Note that even for moderate values of U, the decay is rather small (less than 15% for $U = 5t_h$). (b) The recombined fraction, $1 - N_d^{\rm final}$, vs U/t_h for $8t_h \leq U \leq 40t_h$. $1 - N_d^{\rm final}$ scales as t_h^2/U^2. For $U/t_h = 40$, the recombination is negligible and the system is in the strong coupling limit. (c) N_d for $U = 8t_h$ and two chain lengths, $L = 40$ (solid line) and $L = 80$ (dashed line). The results are independent of the system size.

$$+ \; V \sum_{i=1}^{L-1} (\hat{n}_i - 1)(\hat{n}_{i+1} - 1), \qquad (1)$$

where t_h is the hopping integral, and U and V are the on-site and NN Coulomb repulsion, respectively. The rest of the notation is standard. The ground state $|\Psi_0\rangle$ of $\hat{H}$ is calculated using static DMRG [15, 16]. This state has a charge gap at $U \neq 0$, and spin antiferromagnetic quasi-long-range order.

Light excitation of solids is a complex process in which an energetic electron-hole pair is created by absorbing a photon. In general, the first pair created involves wave-functions not included in the Hubbard model which only takes into account a narrow window around the Fermi level. In most solids, these "hot" electrons and holes quickly dissipate energy into phonons until they reach the quasiparticle energy minimum. Having opposite charge, they find each other because of the long-range part of the Coulomb interaction. We are not modelling the evolution of the state that results from the initial absorption of light. Instead, our goal is to investigate whether the electron and hole will recombine non-radiatively when they find each other. We model this situation by creating an excited state $|\Psi_e\rangle$ formed by a hole and a doubly-occupied-site on two neighboring sites at the center of the chain: $|\Psi_e\rangle = h^\dagger_{L/2} d^\dagger_{L/2+1} |\Psi_0\rangle$, where $h_i^\dagger = (1/\sqrt{2}) \sum_\sigma c_{i\sigma}(1 - n_{i\bar{\sigma}})$ and $d_i^\dagger = (1/\sqrt{2}) \sum_\sigma c^\dagger_{i\sigma} n_{i\bar{\sigma}}$ create a holon and a doublon, respectively [19]. Nearest-neighbors holon and doublon is the most favorable case for an eventual recombination. This state does not correspond to the extended state that light creates but to one that can form after multiple collisions with the lattice. $|\Psi_e\rangle$ is time-evolved under $\hat{H}$, $|\Psi(t)\rangle = e^{-i\hat{H}t}|\Psi_e\rangle$. Due to the third term in $\hat{H}$, the holon and doublon experience an attraction V. However, the system will try to equilibrate by delocalizing the excitation via the kinetic energy term in $\hat{H}$. In the results shown, the measurements are done on $|\Psi(t)\rangle$. To time-evolve the many-body wave-function, the Suzuki-Trotter (ST) decomposition version of TDDMRG is employed [17, 18]. Unless stated otherwise, we use L=40, M=200 DMRG states, t_h=0.2, and the ST time step τ=0.05 [20].

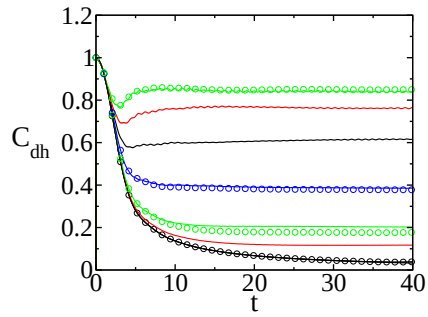

FIG. 2: Time-evolution of the NN holon-doublon correlation function C_{dh} in the strong coupling limit ($U = 40t_h$) for $V/t_h = 0, 0.5, 1.0, 2.0, 3.0, 4.0$, and 5.0 (bottom to top). C_{dh} saturates at a finite value, i.e. a bound state is formed, for any $V > 0$. The open circles show the NN charge-charge correlation function in the simplified model of two spinless fermions (see text for details).

Results. To study the decay of the excitation in real time, we follow the time-evolution of the total double occupation $N_d = \sum_i n_i^d = \sum_i \langle \hat{n}_i^d \rangle = \sum_i \langle \hat{n}_{i\uparrow} \hat{n}_{i\downarrow} \rangle$ [21]. In the results for N_d, and the correlation function shown below, the corresponding ground state value is subtracted. Figure 1(a) shows the time evolution of N_d for different values of U/t_h at $V/t_h = 0$. A small portion of the holon-doublon pair recombines at short times, while the remaining fraction survives indefinitely [22]. As U/t_h increases, the holon-doublon recombination becomes negligible, in spite of the availability of the spin excitations channel; in the strong coupling limit, the holon-doublon pair is conserved. Figure 1(b) shows the asymptotic value of the recombined fraction of the pair. For large U/t_h, this fraction scales as t_h^2/U^2 or J/U, where J=$4t_h^2/U$ is the effective spin coupling. This confirms that the recombination does involve spin excitations in the magnetic background. However, while several spin excitations could be created leading to the decay of most of the holon-doublon pair, it is surprising that their number, proportional to the slope of the curve, is small. This is mainly due to the 1D nature of the system, that allows for holons and doublons to freely propagate even in a spin staggered background, as opposed to the well-known trapping of holes in 2D antiferromagnetic backgrounds due to "string" excitations [23]. Figure 1(c) shows N_d for two different chain lengths with L=40 and 80. The results are nearly identical indicating that the holon-doublon recombination is independent of the system size. Overall, Fig. 1 indicates that the mechanism of the holon-doublon decay into spin excitations is inefficient, and a major fraction of such a pair survives even for moderate values of U/t_h.

It is also interesting to study the nature of the holon-doublon interaction, in particular the formation of a bound state. For this purpose, we measure the NN holon-doublon

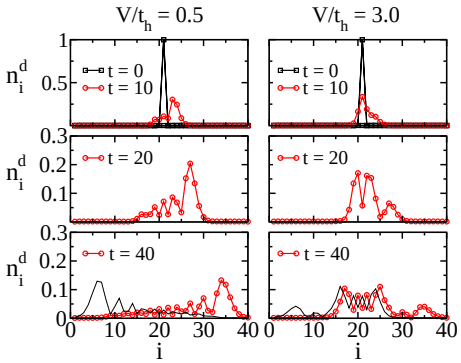

FIG. 3: Doublon propagation in space, in the strong coupling limit ($U = 40t_h$). For $V = 0.5t_h$, most of the doublon propagates to the right (i.e. most of its wave-function is in continuum states). For $V = 3t_h$, the major portion forms an excitonic wave-packet. The transition from the small to the large V behavior occurs at $V = 2t_h$. The holon motion, shown in the lowest two panels, is the reflection of the doublon motion, around the chain center.

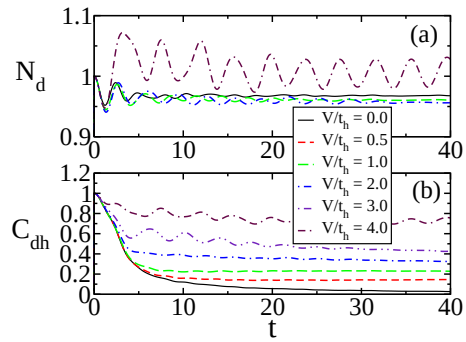

FIG. 4: (a) N_d and (b) C_{dh} for U/t_h=12 and different couplings V/t_h. The final value of N_d shows a nonmonotonic dependence with V/t_h suggesting a competition between two tendencies. Note, however, that the changes are small for the values of V/t_h used. C_{dh} shows the same behavior as in the strong coupling limit. Two plots were deleted from the upper panel for clarity.

correlation function $C_{dh} = \sum_i \langle \hat{n}_i^h \hat{n}_{i+1}^d + \hat{n}_i^d \hat{n}_{i+1}^h \rangle$. Although this correlation function beyond NN can be finite (i.e. the average holon-doublon distance can be larger than 1.0), a finite C_{dh} indicates the formation of a bound state. In the strong-coupling limit, the Hamiltonian reduces to an effective two-body problem, namely two spinless fermions on a tight-binding chain with NN *attraction* V. Previous studies in this limit [13] suggest that a bound state at $K = \pm\pi$ is formed for any $V > 0$; whereas for $K = 0$, a bound state is formed only if $V \geq 2t_h$, where $K = k_d + k_h$ is the total wave-vector of the holon-doublon pair. The exciton has the dispersion $E(K) = U - V - (4t_h^2/V)\cos^2(K/2)$. Our results agree with the above analysis. However, since the two wave-packets contain all possible wave-vectors, the holon-doublon wave-function is expected to split into bound and continuum states depending on V/t_h. Figure 2 shows the time-evolution of C_{dh} in the strong coupling limit for different values of V/t_h. As expected for $V/t_h = 0$, C_{dh} decays to zero at long times i.e. no bound state is formed. For nonzero V/t_h's, C_{dh} shows a clear saturation. For large V/t_h, the saturation value approaches 1.0, i.e. the holon and doublon remain bound at NN sites. For comparison, an effective model of two spinless fermions on a tight-binding chain with NN attraction V was also studied. The initial state, with the two particles at NN sites, is time-evolved exactly under the simplified Hamiltonian, and the NN charge-charge correlation function is calculated. The exact results of the simplified model (shown in Fig. 2) are in very good agreement with the full model TD-DMRG results.

Figure 3 shows the doublon propagation in real space. For a small V, such as $V = 0.5t_h$, most of the wave-packet propagates to the right [24], suggesting that a major fraction of the initial holon-doublon wave-function was in continuum states. The motion of the holon is simply the reflection of the doublon motion around the center of the chain. Note that, in principle, the holon and doublon should move symmetrically in both directions. However, the movement to the left is prevented by energy conservation which forbids these particles from crossing each other via a virtual recombined state. In other words, the holon acts as a hard-wall potential causing the doublon to move in one direction (similar arguments hold for the holon motion). Note that, in addition to the dominant fraction that moves in one direction, there is a long tail of small weight that moves in the other direction. This tail contains a mixture of continuum and bound states of finite K, and this behavior is observed for $0 \leq V < 2t_h$. For larger V, such as $V = 3t_h$, a smaller fraction of the doublon propagates to the right. The dominant part forms a symmetric wave-packet that remains centered at the same site. Results for other values of V/t_h show that the transition from the small to the large V regimes occurs at $V = 2t_h$ [25]. Note that for $V > 2t_h$, a bound state can be formed for any K. Thus, the symmetric wave-packet observed is a mixture of bound states, with all values of K. The bound and continuum states are clearly separated in space for $V > 2t_h$. Even though C_{dh} increases monotonically as V/t_h is increased, note that the doublon propagation in real space falls into two distinct regimes of small and large V/t_h. From the practical point of view, the amount of charge that can be collected at the ends of the chain is not affected by the bound state formation as long as $V < 2t_h$.

The results shown above remain valid as couplings are reduced. Figure 4 shows N_d and C_{dh} for U/t_h=12 and several V/t_h's. The values of V are chosen such that the system is in the Hubbard insulator regime and far from the charge-density-wave (CDW) instability: the transition between the two regimes occurs at V=$U/2$, i.e. V=$6t_h$ in this case [26]. The final value of N_d shows a non-monotonic behavior as a function of V/t_h. This can be understood as the result of the competition between two tendencies. On one hand, for a finite V the energy added to the system upon creating the holon-doublon pair is $U - V$, to zeroth order in t_h. That is, at large V less energy is supplied to the system, thus N_d can relax to smaller values. On the other hand, V increases the CDW ten-

dency in the ground state. And as energy is supplied to the system (by creating the holon-doublon pair), the weight of the higher energy states (the CDW states in this case) increases, thus increasing N_d. Note, however, that the effect of V on N_d is small as long as the system is in the Hubbard insulator regime. C_{dh}, on the other hand, exhibits the same behavior as in the strong coupling limit: a bound state is formed for any $V > 0$. The holon and doublon propagation in space is qualitatively the same as in the strong coupling case (Fig. 3).

Conclusion. We studied the time-evolution of a holon-doublon pair in a 1D extended Hubbard model. The naively expected decay mechanism of the holon-doublon pair to spin excitations is shown to be inefficient, particularly at large U/t_h, and the pair survives for long times [27]. Depending on the value of the NN Coulomb repulsion, the holon-doublon wave-function splits into bound and continuum states. Although a bound state can be formed for any finite NN repulsion, there is a qualitative difference in the real-space propagation between the weak and strong V regimes. It is very important to remark that much of the above results arise from the 1D nature of the problem. The spin background affects much less the holon and doublon propagation in 1D than in higher dimensions [28], where antiferromagnetic links are broken in the direction perpendicular to their movement creating "strings" [23]. Thus, the decay by spin excitations of the holon-doublon pair in 1D is expected to be less likely than in higher dimensions. For these reasons, the main conclusion of our present theoretical effort is that 1D Mott-Hubbard insulators could potentially join semiconductors and polymers as gapped materials of potential relevance for solar cell devices.

K.A. and F.R. thank C. Batista and I. Ivanov for useful discussions. K.A., F.R., I.G., and E.D. were supported by NSF grant DMR-0706020 and the Div. of Mat. Science and Eng., U.S. DOE under contract with UT-Battelle, LLC. LANL is supported by US DOE under Contract No. W-7405-ENG-36.

[1] Y. Tokura and N. Nagaosa, Science **288**, 462 (2000).
[2] H. Kishida *et al.*, Nature **405**, 929 (2000); H. Kishida *et al.*, Phys. Rev. Lett. **87**, 177401 (2001); H. Matsueda *et al.*, Phys. Rev. B **71**, 153106 (2005).
[3] E. Dagotto, Science **309**, 257 (2005).
[4] K. A. Bertness *et al.*, Appl. Phys. Lett. **65**, 989 (1994).
[5] DOE BES Report "Basic research needs for solar energy utilization," April 18-21, 2005. `http://www.sc.doe.gov/bes/reports/files/SEU_rpt.pdf`
[6] J. Y. Kim *et al.*, Science **317**, 222 (2007); I. Gur *et al.*, Science **310**, 462 (2005); M. Law *et al.*, Nature Materials **4**, 455 (2005).
[7] "Photovoltaic System Design" in *Encyclopedia of Physical Science and Technology* Ed. R. A. Meyers, Academic Press (2002).
[8] A. Goetzberger *et al.*, Mat. Science and Eng. R **40**, 1 (2002).
[9] D. G. Shchukin *et al.*, Int. J. of Photoenergy **1**, 65 (1999).
[10] A. Bhattacharya *et al.*, Appl. Phys. Lett. **90**, 222503 (2007).
[11] D. H. Lowndes *et al.*, Science **273**, 898 (1996).
[12] E. Jeckelmann *et al.*, Phys. Rev. Lett. **85**, 3910 (2000); K. Tsutsui *et al.*, Phys. Rev. B **61**, 7180 (2000); F. H. Essler *et al.*, ibid. **64**, 125119 (2001); E. Jeckelmann, ibid., **67**, 075106 (2003).
[13] F. B. Gallagher and S. Mazumdar, Phys. Rev. B **56**, 15025 (1997); W. Barford, ibid. **65**, 205118 (2002); F. Gebhard *et al.*, Phil. Mag. B **75**, 47 (1997).
[14] M. Ono *et al.*, Phys. Rev. Lett. **95**, 087401 (2005).
[15] S. R. White, Phys. Rev. Lett. **69**, 2863 (1992); Phys. Rev. B **48**, 10345 (1993).
[16] K. Hallberg, Adv. Phys. **55**, 477 (2006); U. Schollwöck, Rev. Mod. Phys. **77**, 259 (2005).
[17] S. White and A. Feiguin, Phys. Rev. Lett. **93**, 076401 (2004).
[18] A. J. Daley *et al.*, J. Stat. Mech.: Theory Exp. (2004), P04005.
[19] The definition of $h^\dagger$ and $d^\dagger$ assumes that the probability of double occupancy is small in the ground state. This regime, intermediate and large U/t_h, is the focus of our effort here.
[20] $\hbar$ is set to 1 and time is shown in units of $1/5t_h$.
[21] The total hole occupation $N_h = \sum_i \langle (1-\hat{n}_{i\uparrow})(1-\hat{n}_{i\downarrow})\rangle$ is equal to N_d due to the particle-hole symmetry of the model.
[22] The time scale of the recombination is roughly proportional to $1/U$.
[23] E. Dagotto, Rev. Mod. Phys. **66**, 763 (1994).
[24] The velocity of the doublon is what we expect for the used t_h.
[25] K. A. Al-Hassanieh *et al.*, in preparation.
[26] E. Jeckelmann, Phys. Rev. Lett. **89**, 236401 (2002).
[27] For many excitons, the recombination could occur by the transfer of energy from one exciton to another. The efficiency of this mechanism will be tested in future investigations.
[28] C. Kim *et al.*, Phys. Rev. Lett. **77**, 4054 (1996).